

Contribution from the Department of Chemistry, University of Florence, Florence, Italy, and Departement de Recherche Fondamentale, Centre d'Etudes Nucleaires de Grenoble, Grenoble, France

Structure and Magnetic Properties of a Chain Compound Formed by Copper(II) and a Tridentate Nitronyl Nitroxide Radical

Andrea Caneschi,^{1a} Fabrizio Ferraro,^{1a} Dante Gatteschi,^{*1a} Paul Rey,^{1b} and Roberta Sessoli^{1a}

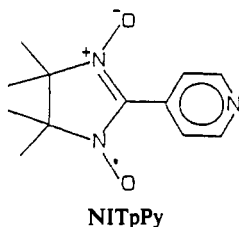
Received October 16, 1990

A novel compound formed by copper(II) and a nitronyl nitroxide radical of formula $[\text{Cu}(\text{hfac})_2]_3(\text{NITpPy})_2$ (where hfac = hexafluoroacetylacetonato and NITpPy = 2-(4-pyridyl)-4,4,5,5-tetramethylimidazoline-1-oxyl 3-oxide) was synthesized. It crystallizes in the monoclinic system, space group $C2/c$, with a 36.540 (9) Å, $b = 23.484$ (7) Å, $c = 21.292$ (6) Å, $\beta = 118.90$ (2)°, and $Z = 8$. The structure consists of chains in which dimeric units $[\text{Cu}(\text{hfac})_2\text{NITpPy}]_2$ are bridged by $\text{Cu}(\text{hfac})_2$ molecules; this is the first compound in which a nitronyl nitroxide radical binds to three metal ions. The magnetic susceptibility was measured in the temperature range 4.2–300 K, and the product χT value as a function of T reaches a broad maximum at about 60 K, due to the predominance of the ferromagnetic exchange interactions between copper(II) and the radical through the short Cu–ON bonds ($J = -80 \text{ cm}^{-1}$) rather than the antiferromagnetic ones through the p -pyridyl nitrogen ($J' = 15 \text{ cm}^{-1}$). A maximum also occurs in the χ versus T curve, at about 13 K. The decrease of χ observed down to the lowest temperature indicates that the ground state is nonmagnetic: this is due to the weak ferromagnetic exchange interaction between copper(II) and the radical through the long Cu–ON bonds. The compound can therefore be considered as a one-dimensional antiferromagnet, and this is also confirmed by single-crystal EPR spectra.

Introduction

We are currently involved in the synthesis of molecular based magnetic materials with high critical transition temperature to magnetic order. The interest in these materials is essentially that of individuating new magnetic behaviors and associations of properties in the perspective to use them in the so-called molecular electronics.^{2–8} With this purpose in mind we decided to investigate the coordinating ability of nitronyl nitroxides, NITR, in which the R group contains additional donor atoms in order to determine the possibility to build extended magnetic structures of dimensionality larger than one. In fact one-dimensional magnetic materials formed by metal ions and NITR radicals have been found to order magnetically below 9 K,^{8–10} and it is clear that in order to increase this limit it is necessary to obtain compounds with stronger interchain interactions.^{11–13}

The radical we are now investigating is NITpPy (where NITpPy = 2-(4-pyridyl)-4,4,5,5-tetramethylimidazoline-1-oxyl 3-oxide).



Compounds in which this radical is bound to metal ions by using

- (1) (a) University of Florence. (b) Centre d'Etudes Nucleaires de Grenoble.
- (2) Kahn, O. *Angew. Chem., Int. Ed. Engl.* **1985**, *24*, 834.
- (3) Breslow, R. *Pure Appl. Chem.* **1982**, *54*, 927.
- (4) Iwamura, H. *Pure Appl. Chem.* **1986**, *58*, 187.
- (5) Miller, J. S.; Epstein, A. J.; Reiff, W. R. *Acc. Chem. Res.* **1988**, *21*, 114.
- (6) Miller, J. S. *Adv. Mater.* **1990**, *2*, 98. Miller, J. S. *Adv. Mater.* **1990**, *2*, 378.
- (7) Caneschi, A.; Gatteschi, D.; Sessoli, R.; Rey, P. *Acc. Chem. Res.* **1989**, *22*, 392.
- (8) Caneschi, A.; Gatteschi, D.; Renard, J. P.; Rey, P.; Sessoli, R. *Inorg. Chem.* **1989**, *28*, 1976.
- (9) Caneschi, A.; Gatteschi, D.; Renard, J. P.; Rey, P.; Sessoli, R. *Inorg. Chem.* **1989**, *28*, 3314.
- (10) Caneschi, A.; Gatteschi, D.; Renard, J. P.; Rey, P.; Sessoli, R. *Inorg. Chem.* **1989**, *28*, 2940.
- (11) Pei, Y.; Verdager, M.; Kahn, O.; Sletten, J.; Renard, J. P. *J. Am. Chem. Soc.* **1986**, *108*, 7428.
- (12) Nakatani, K.; Carriat, J. Y.; Journaux, Y.; Kahn, O.; Lloret, F.; Renard, J. P.; Pei, Y.; Sletten, J.; Verdager, M. *J. Am. Chem. Soc.* **1989**, *111*, 5739.
- (13) Miller, J. S.; Epstein, A. J.; Reiff, W. M. *Chem. Rev.* **1988**, *88*, 201.

Table I. Crystallographic Data and Experimental Parameters for $[\text{Cu}(\text{hfac})_2]_3(\text{NITpPy})_2$

formula	$\text{C}_{54}\text{H}_{38}\text{N}_6\text{O}_{16}\text{F}_{36}\text{Cu}_3$	V	15995.4 \AA^3
mol wt	1901.5	Z	8
crust syst	monoclinic	density	1.579 g/cm^3
space group	$C2/c$	μ	7.11 cm^{-1}
a	36.540 (9) Å	temp	$20 \text{ }^\circ\text{C}$
b	23.484 (7) Å	λ	0.7107 \AA
c	21.292 (6) Å	refinement	$R = 0.085$
β	118.90 (2)°	R_w	$= 0.096$

either only the nitrogen atom of the p -pyridyl ring^{14,15} or both the p -pyridyl nitrogen and one oxygen atom of a NO group^{16,17} have been synthesized and characterized. We have now found that NITpPy can bind as a tridentate ligand to copper(II), yielding a compound with an extended structure, and we want to report here its crystal structure and magnetic properties.

Experimental Section

Synthesis. $\text{Cu}(\text{hfac})_2$, where hfac = hexafluoroacetylacetonate, and NITpPy were prepared as previously described.^{18,19} A 1-mmol amount of $\text{Cu}(\text{hfac})_2$ was dissolved in hot n -heptane, the solution was cooled, and a CH_2Cl_2 solution containing 0.66 mmol of NITpPy was added. The mixture was stored at room temperature for 5 days, and then light green well-shaped crystals were collected and well analyzed for $[\text{Cu}(\text{hfac})_2]_3(\text{NITpPy})_2$. Anal. Calcd for $\text{C}_{54}\text{Cu}_3\text{F}_{36}\text{H}_{38}\text{N}_6\text{O}_{16}$: C, 34.09; H, 2.00; N, 4.42. Found: C, 33.92; H, 1.98; N, 4.28.

X-ray Structure Determination. X-ray data were collected on an Enraf-Nonius CAD4 four-circle diffractometer with $\text{Mo K}\alpha$ radiation at room temperature. Cell parameters were obtained by a least-squares refinement of the setting angles of 23 reflections in the range $10^\circ \leq \theta \leq 14^\circ$. Experimental parameters are reported in Table SI of the supplementary material and in Table I, in a condensed form. Data were corrected for Lorentz and polarization effects but not for absorption.

The Patterson map revealed the position of two of the three copper atoms of the asymmetric unit; the positions of the other non-hydrogen atoms were obtained by successive Fourier and difference Fourier syntheses using the SHELX76 package.²⁰ Only the copper atoms, the

- (14) Caneschi, A.; Ferraro, F.; Gatteschi, D.; Rey, P.; Sessoli, R. *Inorg. Chem.* **1990**, *29*, 1756.
- (15) Caneschi, A.; Ferraro, F.; Gatteschi, D.; Rey, P.; Sessoli, R. *Inorg. Chem.* **1990**, *29*, 4217.
- (16) Caneschi, A.; Gatteschi, D.; Rey, P.; Sessoli, R. *Inorg. Chim. Acta* **1991**, *184*, 67.
- (17) Unpublished results of this laboratory.
- (18) Lanchem, M.; Wittag, T. W. *J. Chem. Soc. C* **1966**, 2300.
- (19) Ullmann, E. F.; Call, L.; Osiecki, J. H. *J. Org. Chem.* **1970**, *35*, 3623. Davis, M. S.; Morokuma, K.; Kreilick, R. W. *J. Am. Chem. Soc.* **1972**, *94*, 5588.
- (20) Sheldrick, G. SHELX76 System of Computing Program. University of Cambridge, Cambridge, England, 1976. Atomic scattering factors after: Cromer, D. T.; Liberman, D. J. *J. Chem. Phys.* **1970**, *53*, 1891.

Table II. Positional Parameters ($\times 10^4$) and Isotropic Thermal Factors ($\text{\AA}^2 \times 10^3$) for [Cu(hfac)₂]₃(NITpPy)₂^a

	<i>x/a</i>	<i>y/b</i>	<i>z/c</i>	<i>U</i> _{iso} ^b		<i>x/a</i>	<i>y/b</i>	<i>z/c</i>	<i>U</i> _{iso} ^b
Cu1	3255 (1)	2909 (1)	3826 (1)	61 (1)	C16	2775 (6)	1431 (8)	2608 (10)	83 (5)
Cu2	924 (1)	3965 (1)	806 (1)	70 (1)	C17	4214 (9)	2145 (13)	3537 (16)	130 (9)
Cu3	2164 (1)	5138 (1)	4736 (1)	66 (1)	C18	3767 (5)	3619 (7)	5047 (9)	77 (5)
O1	1091 (3)	3496 (5)	2033 (6)	83 (8)	C19	3816 (5)	3255 (7)	5570 (8)	69 (4)
O2	1796 (3)	5034 (4)	3426 (5)	66 (7)	C20	3644 (5)	2740 (7)	5426 (8)	71 (5)
O3	2962 (3)	2244 (4)	3299 (5)	63 (3)	C21	3963 (10)	4220 (13)	5279 (18)	138 (9)
O4	3787 (3)	2649 (4)	3857 (5)	67 (3)	C22	3728 (8)	2383 (11)	6065 (14)	123 (8)
O5	3564 (3)	3576 (4)	4364 (5)	76 (3)	C23	2710 (4)	3927 (6)	1716 (8)	57 (4)
O6	3402 (3)	2499 (4)	4841 (5)	75 (3)	C24	3426 (5)	4015 (7)	2244 (9)	77 (5)
O7	3109 (3)	3208 (4)	2501 (5)	73 (7)	C25	3217 (5)	4615 (7)	1975 (8)	69 (4)
O8	2522 (3)	4787 (4)	1057 (5)	81 (8)	C26	3547 (5)	3705 (7)	1726 (9)	91 (6)
O9	1189 (3)	2352 (4)	1472 (5)	69 (3)	C27	3801 (6)	6014 (8)	8031 (10)	98 (6)
O10	399 (3)	2836 (4)	811 (5)	84 (3)	C28	3224 (6)	4973 (8)	2578 (10)	99 (6)
O11	815 (4)	2426 (5)	-111 (7)	120 (4)	C29	3386 (6)	4952 (8)	1561 (10)	96 (6)
O12	654 (3)	3596 (5)	152 (6)	92 (3)	C30	2287 (4)	3696 (6)	1459 (7)	49 (4)
O13	2412 (3)	4391 (4)	4936 (5)	65 (3)	C31	1944 (4)	4046 (6)	1233 (8)	59 (4)
O14	1691 (3)	4872 (4)	4834 (5)	72 (3)	C32	1546 (5)	3829 (7)	998 (8)	77 (5)
O15	1939 (3)	5905 (4)	4590 (5)	74 (3)	C33	1840 (5)	2911 (6)	1267 (8)	69 (4)
O16	2639 (3)	5394 (4)	4654 (5)	74 (3)	C34	2229 (4)	3115 (6)	1498 (7)	58 (4)
N1	1176 (3)	3982 (5)	2339 (6)	53 (3)	C35	1012 (5)	2020 (7)	1690 (9)	76 (5)
N2	1510 (4)	4704 (5)	3002 (6)	52 (3)	C36	609 (6)	2035 (8)	1595 (10)	91 (5)
N3	2704 (3)	3313 (4)	3508 (5)	46 (3)	C37	350 (6)	2444 (8)	1167 (10)	96 (6)
N4	3070 (4)	3687 (5)	2196 (6)	60 (3)	C38	1299 (9)	1549 (13)	2155 (16)	128 (8)
N5	2789 (4)	4446 (5)	1519 (7)	60 (3)	C39	-113 (14)	2484 (20)	1094 (24)	189 (15)
N6	1492 (3)	3242 (5)	1038 (6)	63 (3)	C40	602 (8)	2630 (12)	-770 (13)	140 (9)
C1	1550 (4)	4180 (5)	2805 (7)	47 (4)	C41	450 (6)	3142 (10)	-967 (11)	105 (6)
C2	828 (5)	4377 (7)	2251 (9)	72 (5)	C42	476 (5)	3537 (8)	-549 (9)	85 (5)
C3	1070 (5)	4914 (7)	2550 (9)	73 (5)	C43	555 (20)	2204 (25)	-1288 (37)	308 (33)
C4	681 (7)	4110 (9)	2790 (12)	126 (7)	C44	280 (13)	4117 (16)	-878 (22)	181 (13)
C5	480 (7)	4364 (9)	1479 (12)	127 (7)	C45	2299 (4)	3977 (5)	5172 (7)	47 (4)
C6	941 (7)	5309 (9)	2979 (12)	130 (8)	C46	1949 (4)	3944 (6)	5250 (8)	62 (4)
C7	1074 (6)	5281 (9)	1920 (11)	113 (7)	C47	1678 (5)	4392 (6)	5084 (8)	65 (4)
C8	1943 (4)	3893 (6)	3048 (7)	49 (4)	C48	2587 (6)	3475 (8)	5378 (10)	78 (5)
C9	2319 (5)	4184 (6)	3313 (8)	66 (4)	C49	1305 (6)	4336 (9)	5204 (11)	84 (5)
C10	2692 (4)	3882 (6)	3535 (7)	56 (4)	C50	2119 (5)	6323 (7)	4493 (8)	70 (4)
C11	2344 (4)	3034 (6)	3237 (7)	56 (4)	C51	2468 (5)	6373 (7)	4487 (8)	76 (5)
C12	1960 (4)	3295 (6)	2996 (7)	59 (4)	C52	2717 (5)	6891 (6)	4553 (8)	69 (4)
C13	3116 (5)	1884 (7)	3022 (8)	74 (5)	C53	1809 (7)	6839 (10)	4292 (13)	102 (7)
C14	3499 (5)	1853 (7)	3080 (8)	73 (5)	C54	3124 (6)	5958 (9)	4501 (12)	85 (5)
C15	3790 (5)	2236 (7)	3491 (8)	70 (5)					

^aStandard deviations in the last significant digits are in parentheses. ^b $U_{iso} = 1/3 \sum_i \sum_j U_{ij} a_i^* a_j^* a_i a_j$.

oxygen atoms of the nitronyl nitroxides, and the fluorine atoms of the hexafluoroacetylacetonates were refined anisotropically due to the large number of parameters compared to the number of reflections, and hydrogen atoms were not introduced. The final least-squares refinement converged to $R = 0.085$. The highest peak in the last difference Fourier map was 0.56 e/\AA^3 and located in proximity of the C2 atom of the pentaatomic ring of one of the two radicals. Atomic positional parameters and isotropic thermal factors for all non-fluorine atoms are listed in Table II. Anisotropic thermal factors are listed in Table SII, while atomic positional parameters and isotropic thermal factors for fluorine atoms are available in Table SV or supplementary material.

Magnetic and EPR Measurements. Magnetic susceptibility was measured in the temperature range 5–300 K by using an automated AZTEC DSM5 susceptometer equipped with an Oxford Instruments CF1200S continuous-flow cryostat and a Bruker B-E15 electromagnet. Diamagnetic corrections were estimated from Pascal's constants. Polycrystalline powder and single-crystal EPR spectra were obtained with a Varian E9 spectrometer at X-band frequency. Variable-temperature spectra were recorded by using an Oxford Instruments ESR9 continuous-flow cryostat. A single crystal of [Cu(hfac)₂]₃(NITpPy)₂ was oriented with the above mentioned diffractometer and was found to have the form of an almost square platelet with largely developed (100) and (100) faces.

Results

Crystal Structure. The compound crystallizes in the monoclinic system, space group $C2/c$. The asymmetric unit consists of a [Cu(hfac)₂]₃(NITpPy)₂ group, shown in Figure 1. The two nonequivalent but very similar NITpPy molecules are coordinated to three copper atoms. The pyridine nitrogen of one radical, N3, binds to Cu1, while the oxygen atoms of the two NO groups, O1 and O2, give long bonds to Cu2 and Cu3 (2.69 and 2.46 Å, respectively). The pyridine nitrogen of the other radical, N6, binds to Cu2, while O7 binds to Cu1 and O8 to Cu3 of a different

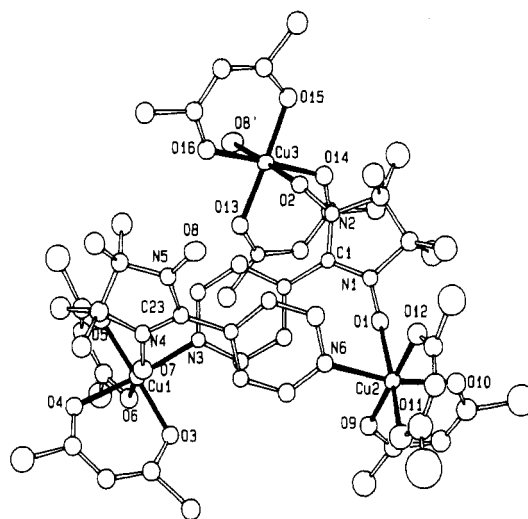


Figure 1. ORTEP view of the asymmetric unit of [Cu(hfac)₂]₃(NITpPy)₂. The fluorine atoms were omitted for clarity. Only the relevant atoms have been labeled in this figure; for the complete labeling, see Figure S1 in the supplementary material.

asymmetric unit. The structure can be schematized as shown in Figure 2: dimeric [Cu(hfac)₂NITpPy]₂ units are bridged by Cu(hfac)₂ molecules to give chains parallel to the *c* crystal axis.

Selected bond distances and angles are presented in Table III. The copper atom of the bridging Cu(hfac)₂ molecule, Cu3, has a distorted octahedral coordination, with the oxygen atoms of two hfac anions bound to the metal ion in the equatorial plane, while

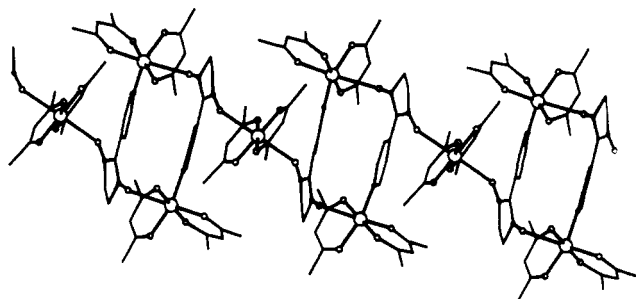


Figure 2. View of the chain structure formed by dimeric $[\text{Cu}(\text{hfac})_2\text{NITpPy}]_2$ units bridged by $\text{Cu}(\text{hfac})_2$ moieties. Fluorine atoms and methyl groups are not reported for the sake of clarity.

Table III. Selected Bond Distances (Å) and Angles (deg)^a

Cu1-O3	1.92 (1)	Cu3-O8'	2.47 (1)
Cu1-O4	2.01 (1)	Cu3-O13	1.93 (1)
Cu1-O5	1.95 (1)	Cu3-O14	1.94 (1)
Cu1-O6	2.18 (1)	Cu3-O15	1.94 (1)
Cu1-O7	2.70 (1)	Cu3-O16	1.92 (1)
Cu1-N3	2.02 (1)	O1-N1	1.28 (2)
Cu2-O1	2.69 (1)	O2-N2	1.26 (1)
Cu2-O9	1.92 (1)	N1-C1	1.32 (2)
Cu2-O10	1.95 (1)	N2-C1	1.33 (2)
Cu2-O11	2.19 (1)	O7-N4	1.27 (2)
Cu2-O12	1.94 (1)	O8-N5	1.28 (1)
Cu2-N6	1.99 (1)	N4-C23	1.34 (2)
Cu3-O2	2.46 (1)	N5-C23	1.37 (2)
O7-Cu1-N3	82.3 (4)	O1-Cu2-N6	83.5 (4)
O6-Cu1-N3	105.5 (4)	O1-Cu2-O12	98.1 (4)
O6-Cu1-O7	168.4 (4)	O1-Cu2-O11	172.3 (4)
O5-Cu1-N3	91.2 (4)	O1-Cu2-O10	80.0 (4)
O5-Cu1-O7	99.8 (4)	O1-Cu2-O9	80.4 (4)
O5-Cu1-O6	88.7 (4)	O15-Cu3-O16	91.6 (5)
O4-Cu1-N3	160.8 (4)	O14-Cu3-O16	179.0 (4)
O4-Cu1-O7	79.1 (4)	O14-Cu3-O15	89.2 (5)
O4-Cu1-O6	93.6 (4)	O13-Cu3-O16	87.4 (5)
O4-Cu1-O5	87.0 (4)	O13-Cu3-O15	176.8 (4)
O3-Cu1-N3	90.1 (4)	O13-Cu3-O14	91.9 (4)
O3-Cu1-O7	80.0 (4)	O8'-Cu3-O16	94.4 (4)
O3-Cu1-O6	91.2 (5)	O8'-Cu3-O15	93.9 (4)
O3-Cu1-O5	178.6 (5)	O8'-Cu3-O14	84.9 (4)
O3-Cu1-O4	91.7 (4)	O8'-Cu3-O13	83.1 (4)
O12-Cu2-N6	92.1 (5)	O2-Cu3-O16	87.1 (4)
O11-Cu2-N6	97.4 (6)	O2-Cu3-O15	87.3 (4)
O11-Cu2-O12	89.6 (5)	O2-Cu3-O14	93.6 (4)
O10-Cu2-N6	163.4 (5)	O2-Cu3-O13	95.7 (4)
O10-Cu2-O12	87.8 (5)	O2-Cu3-O8'	178.0 (4)
O10-Cu2-O11	99.2 (5)	Cu2-O1-N1	143 (1)
O9-Cu2-N6	88.3 (5)	Cu1-O7-N4	133 (1)
O9-Cu2-O12	178.3 (5)	Cu3-O2-N2	133 (1)
O9-Cu2-O11	92.0 (5)	Cu3-O8'-N5'	135 (1)
O9-Cu2-O10	91.4 (5)		

^aStandard deviations in the last significant digit are in parentheses.

the axial positions are occupied, at greater distances (2.46–2.47 Å), by the oxygen atoms O2 of a nitronyl nitroxide and O8' of a radical that belongs to a different asymmetric unit. Cu1 and Cu2 have an approximately square-pyramidal coordination of two hfac anions and the pyridine nitrogen of a NITpPy radical, with the axial position occupied by an oxygen of the hfac ligand at a larger distance than the other ones (2.18–2.19 Å vs equatorial distances in the range 1.92–2.02 Å). The sixth donor atom is much more distant (2.69–2.70 Å), in a position almost opposite to the other axial donor atom (O6–Cu1–O7 = 168.4°; O1–Cu2–O11 = 172.3°). The planes of the two chelated rings formed by copper atoms and by the hfac anions are almost perpendicular to each other in both copper sites. The bond distances of the pyridine and hfac anions are similar to those observed in $\text{Cu}(\text{hfac})_2\text{Py}_2$ adducts.²¹ The bond distances and angles in the radicals agree with those measured in other adducts of metal ion

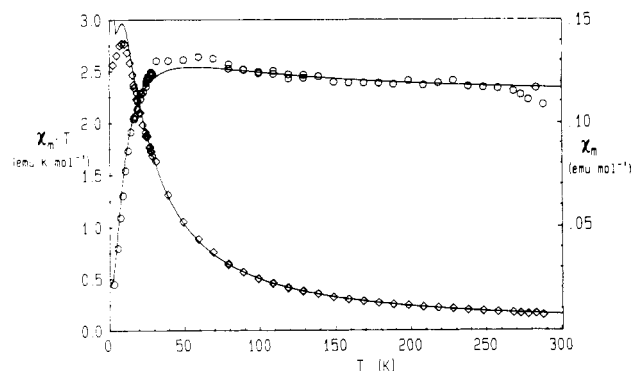


Figure 3. Temperature dependence of χ_m (\diamond) and $\chi_m T$ (\circ) for $[\text{Cu}(\text{hfac})_2]_3(\text{NITpPy})_2$. The solid lines represent the values calculated with the parameters of the text.

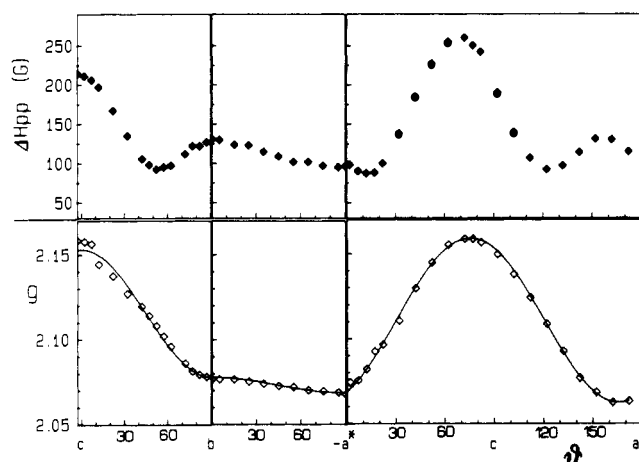


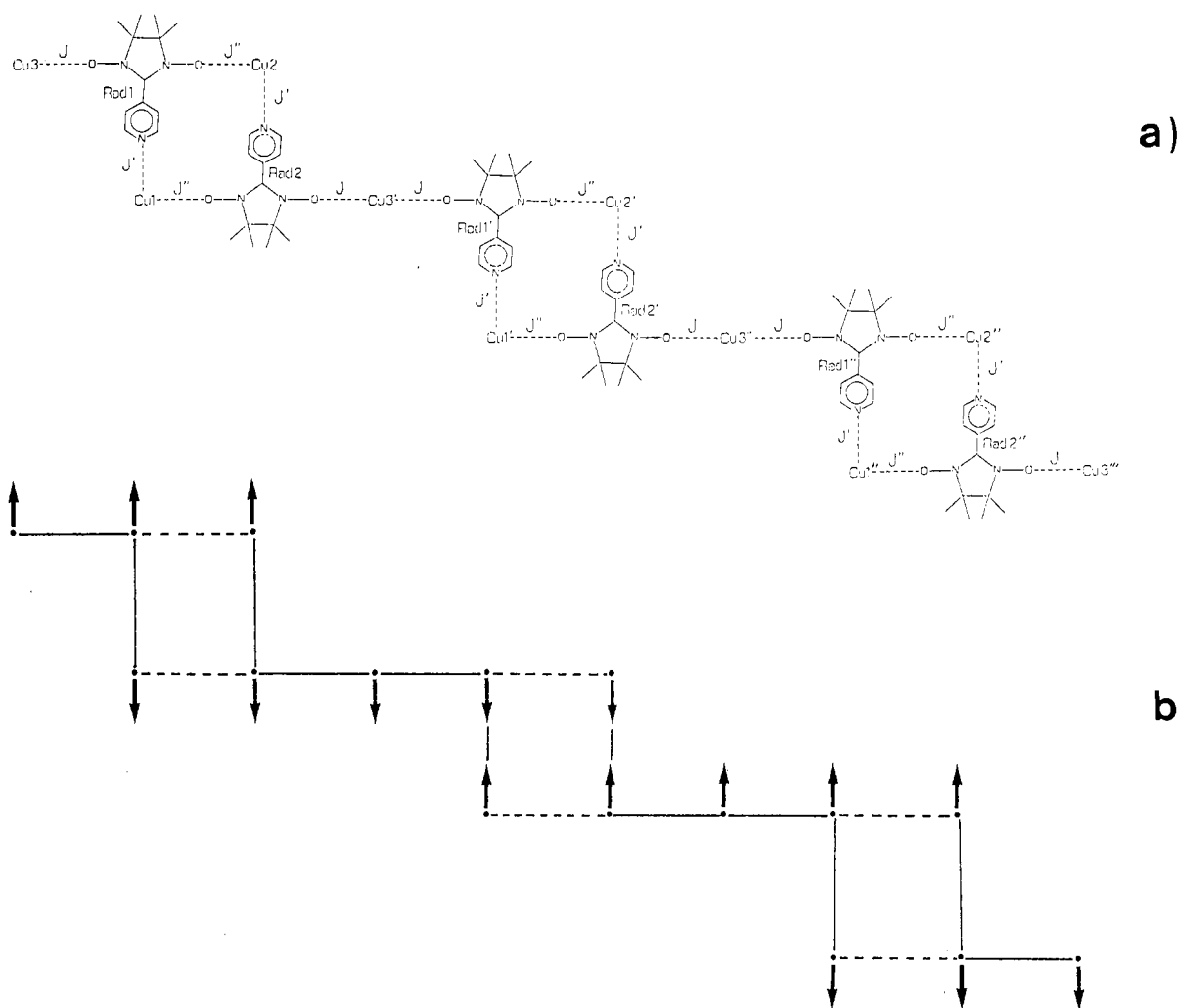
Figure 4. Angular dependence of the observed g values (\diamond) and line widths (\blacklozenge) in the rotations around a^* , c , and b axes at room temperature. The solid lines correspond to the calculated g values according to the Kramers formula; see text.

β diketonates.²² In both the radicals of the asymmetric unit the conjugation planes (defined by the atoms O7–N4–C23–N5–O8 for one radical and O1–N1–C2–N2–O2 for the other) and the p -pyridyl rings are not coplanar, forming a dihedral angle of 21.5° and 25.3° for the two cases, respectively. The two radicals are stacked, with the p -pyridyl rings, which are separated by an average distance of about 3.6 Å, and form an angle of 9.7°. The stacking of the p -pyridyl groups in the compounds of the NITpPy radical is rather frequent: in particular the same rectangular cluster formed by two metal ions and two NITpPy radicals present in $[\text{Cu}(\text{hfac})_2]_3(\text{NITpPy})_2$ also occurs in a gadolinium(III) and in a manganese(II) compound.^{16,17}

Magnetic and EPR Data. The temperature dependence of χ and χT for $[\text{Cu}(\text{hfac})_2]_3(\text{NITpPy})_2$ is shown in Figure 3. The room-temperature value of χT , 2.33 emu K mol⁻¹, is slightly larger than expected (2.05 emu K mol⁻¹) for five $S = 1/2$ spins, two of which (the radicals) have $g = 2.0$ and the others (the copper ions) have $g = 2.15$. χT increases on decreasing temperature, reaching a round maximum at about 60 K, corresponding to $\chi T = 2.63$ emu K mol⁻¹. Below 30 K χT decreases drastically, reaching the value of 0.45 emu K mol⁻¹ at liquid-helium temperature. On the other hand, magnetic susceptibility increases on lowering temperature to about 10 K and decreases at lower temperature.

Polycrystalline powder EPR spectra were recorded at X-band frequency at both room and liquid-helium temperatures. In both cases a unique line of width 125 and 215 G, respectively, at room temperature and 4.2 K, is observed at $g = 2.10$. Single-crystal spectra were recorded by rotating around the b , c , and $a^* = b \times c$ at room and liquid-helium temperatures. Since only one signal was observed for every orientation of the crystal relative to the

Scheme I



external magnetic field, the angular dependence of the g values was followed with the formulas appropriate to Kramers doublets,²³ and the room temperature results are shown in Figure 4, as well as the line widths. The principal values and direction cosines of the g tensor are reported in Table IV. The fact that only one signal was observed in every crystal orientation shows that the asymmetric units, which are reported by glide planes and are therefore magnetically nonequivalent, are averaged by exchange interactions in the crystal.²⁴

The g_2 component of the tensor is directed along the b axis, while the g_1 and g_3 components are in the ac plane, g_1 forming an angle of 14.7° with the c axis. For an isolated copper(II) ion in an octahedral or square-pyramidal coordination, the direction of the maximum g -value component is expected to be that of the longer bond,²⁴ while the g tensor of the radical can be taken as isotropic. Therefore, the direction of the g_1 component in this exchange-coupled spin system at high temperature is expected to be the average between those of the maximum g component for the single copper(II) spins. In computing the average, we have to consider not only the three copper spins in the asymmetric unit but also those of the adjacent one, which are magnetically not equivalent. The direction cosines for g_1 estimated in this way are reported in Table IV, and they agree with those obtained from the experimental data within 2.5° .

The line widths show a magic angle behavior of the type $\Delta H \propto (1 - 3 \cos^2 \theta)^n$ when plotted as a function of the angle θ between

Table IV. Experimental and Calculated Principal Values and Direction Cosines of the g Tensor in the a^*bc Reference Frame^a

g	directions	
	experimental	calculated
$g_1 = 2.16$	0.2532	0.2952
	0.0068	0.0000
	0.9674	0.9554
$g_2 = 2.08$	0.9671	
	0.0225	
$g_3 = 2.06$	-0.2533	
	0.0235	
	-0.9997	
	0.0009	

^a The experimental parameters are obtained from the fitting of the spectra with the formulas appropriate to the Kramers doublets. The calculated values are obtained as described in the text.

the c axes and the external magnetic field. No such behavior is retained in the a^*b plane. Noteworthy is that the maximum in the line width is observed within error parallel to the g_1 component of the g tensor.

On decreasing temperature the spectra remain similar to those of room temperature, showing only a large increase in the line widths below 10 K. The principal g values at 4.2 K are $g_1 = 2.14$, $g_2 = 2.10$, and $g_3 = 2.08$; the directions are the same as at room temperature. There is no evidence of half-field transition at any orientation, neither at room temperature nor at 4.2 K.

Discussion

The choice of the model for the interpretation of the magnetic data of [Cu(hfac)₂]₃(NITpPy)₂ is rather complicated because of the large number of magnetic interactions that should be, in

(23) Schonland, D. S. *Proc. Phys. Soc.* **1959**, *73*, 788.

(24) Bencini, A.; Gatteschi, D. In *Transition Metal Chemistry*, Marcel Dekker, Inc.: New York, 1982; Vol. 8.

(25) Bencini, A.; Gatteschi, D. *EPR of Exchange Coupled Systems*, Springer-Verlag: Berlin, 1990.

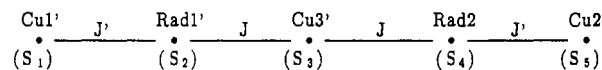
principle, taken into account. However, the comparison with the well-understood magnetic properties in other copper-radical complexes^{22,26} offers a safe guide to unravel the magnetic properties of $[\text{Cu}(\text{hfac})_2]_3(\text{NITpPy})_2$.

In Scheme 1a we show the skeleton of the chains including only copper ions and radicals. We put to zero the cross-interactions between Cu1–Cu2 and Rad1–Rad2, which are expected to be small, since both the NO groups and the copper ions are well separated from each other (the shortest interrads distance is 6.76 Å, and the Cu1–Cu2 distance is 7.81 Å). The interaction between the NITpPy radical and copper(II) through the *p*-pyridyl ring was found to be antiferromagnetic and rather large ($J' \approx 20 \text{ cm}^{-1}$)¹⁴ and has to be taken into account. Cu3 is axially coordinated by the oxygens of two radicals with Cu–O distances (2.46 and 2.47 Å) that are similar to those found in other compounds with axial interactions between copper(II) and NITR radicals, where the coupling constants were found to be ferromagnetic with J values in the range 25–60 cm^{-1} .^{22,26} On the other hand, the longer NO–Cu bonds observed between Rad1 and Cu2 and between Rad2 and Cu1 (2.69 and 2.70 Å) suggest that the corresponding magnetic coupling constants, J'' , are ferromagnetic and small. In this description we have assumed the same coupling constants for the two nonequivalent radicals; however, the close similarity of their coordination allows us to neglect the differences at least in a semiquantitative treatment.

This pattern of exchange interactions suggests that $[\text{Cu}(\text{hfac})_2]_3(\text{NITpPy})_2$ must behave as a one-dimensional magnetic material. In particular although there are more ferromagnetic coupling constants than antiferromagnetic ones, the simple spin arrangement of Scheme 1b shows that at sufficiently low temperature $[\text{Cu}(\text{hfac})_2]_3(\text{NITpPy})_2$ must behave as a one-dimensional antiferromagnet. In fact, as a consequence of the weak interactions J'' , which couple different asymmetric units, the ground state is such that the orientation of every spin is opposite to that of the corresponding spin reported by the glide plane in the adjacent asymmetric unit. The EPR spectra confirm the one-dimensional nature of the compound, both with the g values, which indicate exchange interaction between the magnetically nonequivalent units, and with the angular dependence of the line width, which has the magic angle behavior expected for one-dimensional magnetic materials.^{27,28}

The chain structure of $[\text{Cu}(\text{hfac})_2]_3(\text{NITpPy})_2$ is magnetically rather complicated. In fact we have at least three different kinds of spins (Cu1, Rad1, and their analogous Cu2 and Rad2, plus Cu3). We can describe the chain as formed by rings of four spins connected by copper ions. Although many different one-dimensional materials have been taken into consideration up to now,^{29,30} we do not see any simple way to calculate the magnetic properties of such a type of chain. Therefore, we must try to introduce some approximations in order to have a semiquantitative estimation of the magnetic properties of $[\text{Cu}(\text{hfac})_2]_3(\text{NITpPy})_2$.

Assuming that J'' is small, we may consider that the high-temperature magnetic data are determined by the other coupling constants. Therefore, we can take into consideration clusters of five spin with the following coupling scheme:



The associated Heisenberg exchange Hamiltonian is

$$H = J(S_3S_2 + S_3S_4) + J'(S_2S_1 + S_4S_5)$$

The increases of χT on decreasing temperature in the range 300–60 K indicates that the strongest coupling constant is the ferromagnetic one, J . In fact, in this hypothesis, neglecting for the moment J' , we may expect that the low-temperature limit of χT corresponds to the sum of a quartet (the central copper ion ferromagnetically coupled to the two radicals) plus two doublets (the external uncorrelated copper ions). The plateau observed between 60 and 30 K corresponds well to this limit. The observed susceptibility can be satisfactorily reproduced with $J = -80 \text{ cm}^{-1}$, $J' = 15 \text{ cm}^{-1}$, and $g = 2.17$, as can be seen in Figure 3, where the calculated χ and χT values are reported. The agreement is rather good down to about 13 K, but below this temperature the measured χ and χT values are lower than the calculated ones and in particular the experimental susceptibility χ does not diverge. In fact in our simple model we have neglected the weak ferromagnetic interactions J'' through the long Cu–ON bonds, which are responsible of the nonmagnetic ground state and whose effects become evident only at low temperature.

It is interesting to notice the unusual behavior of the calculated susceptibility for the cluster of five spins, which goes through a maximum at about 10 K, decreases slightly, and then increases again. This is due to the fact that below 30 K the χ vs T curve must pass from the values expected for a quartet plus two doublets, as explained above, to those expected for a doublet, which is the ground state when J' is taken into account.

Conclusion

$[\text{Cu}(\text{hfac})_2]_3(\text{NITpPy})_2$ showed that NITpPy can act as a tridentate ligand toward transition-metal ions, although the two NO groups yield only semicoordinative bonds with copper. We decided to use NITpPy as a ligand just in the hope to observe tridentate behavior; therefore, in this respect $[\text{Cu}(\text{hfac})_2]_3(\text{NITpPy})_2$ has been a success. Further magnetic coupling is transmitted through all the three donor centers. However, our final goal was that of designing materials whose magnetic dimensionality is larger than one, and in this sense $[\text{Cu}(\text{hfac})_2]_3(\text{NITpPy})_2$ is disappointing, because it behaves as a one-dimensional magnetic material. Also, our goal is that of designing ferromagnetic materials, and although the $[\text{Cu}(\text{hfac})_2]_3(\text{NITpPy})_2$ units, which have a ground state with one unpaired electron, are connected through ferromagnetic interactions, the material behaves as an antiferromagnetic chain. This shows how crucial is the connectivity between the magnetic centers in order to obtain ferromagnetic behavior.

Finally, the other interesting feature of $[\text{Cu}(\text{hfac})_2]_3(\text{NITpPy})_2$ is that there are two different copper ions and in principle one of them might be substituted by another metal ion, yielding novel magnetic behaviors. We are currently investigating systems of this kind.

Acknowledgment. The financial support of the CNR, of the Progetto Finalizzato "Materiali Speciali per Tecnologie Avanzate", and of MURST is gratefully acknowledged.

Supplementary Material Available: Tables SI and SII, listing experimental and crystallographic data and anisotropic thermal factors for all atoms, Tables SIII and SIV, listing bond lengths and angles, Table SV, listing positional parameters and isotropic thermal factors of the fluorine atoms, and Figure S1, showing an ORTEP structure of the completely labeled asymmetric unit (14 pages); a table of observed and calculated structure factors (20 pages). Ordering information is given on any current masthead page.

- (26) Caneschi, A.; Gatteschi, D.; Grand, A.; Laugier, J.; Pardi, L.; Rey, P. *Inorg. Chem.* **1988**, *27*, 1031. Cabello, C. I.; Caneschi, A.; Carlin, R. L.; Gatteschi, D.; Rey, P.; Sessoli, R. *Inorg. Chem.* **1990**, *29*, 2582.
 (27) Richards, P. M. In *Local Properties at Phase Transitions*, Editrice Compositori: Bologna, Italy, 1975.
 (28) Gatteschi, D.; Sessoli, R. *Magn. Res. Rev.* **1990**, *15*, 1.
 (29) De Jongh, L. J.; Miedema, A. R. *Adv. Phys.* **1974**, *23*, 1.
 (30) Hatfield, W. E.; Estes, W. E.; Marsh, W. E.; Pickens, M. W.; ter Haar, L. W.; Weller, R. R. In *Extended Linear Chain Compounds*, Miller, J. S., Ed.; Plenum Press: New York, 1983; Vol. 3, p 43.